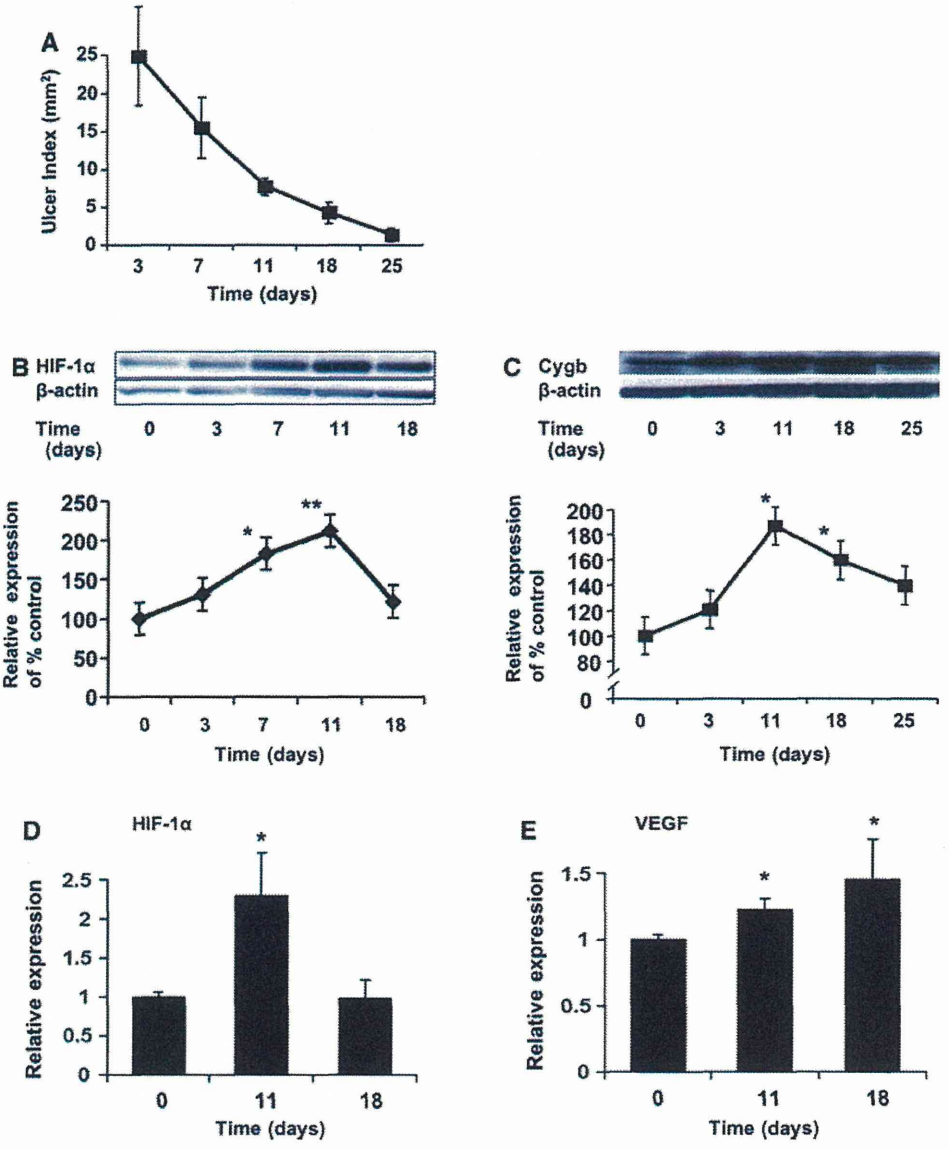

Fig. 2 HIF-1α and Cygb protein expression in an experimental gastric ulcer model. Changes in gastric ulcer size (**a**), expression of HIF-1α protein (**b**), and Cygb protein (**c**) in the ulcerated tissues. HIF-1α protein was significantly increased on day 7 after the production of gastric ulcer (1.83 ± 0.11 folds, $p < 0.05$ vs. control) and sustained up to day 11 (2.12 ± 0.19 folds, $p < 0.01$), which corresponded to the early phase of healing stage. In contrast, Cygb protein was significantly increased on days 11 and 18 (1.87 ± 0.13 and 1.60 ± 0.06 folds, respectively, $p < 0.05$), which corresponded to the late phase of healing. Interestingly, HIF-1α was not significantly increased on day 18 whereas Cygb was increased. There was a difference between HIF-1α and Cygb protein expression in the time phase. Each value represents the mean ± SEM ($N = 5$–6). $^{*}p < 0.05$ and $^{**}p < 0.01$ versus control. mRNA expressions of HIF-1α (**d**) and VEGF (**e**) in the ulcerated gastric tissues. Expression of HIF-1α peaked on day 11. In contrast, VEGF expression was gradually increased from day 11 to 18. VEGF expression peaked at day 18. Each value represents the mean ± SEM ($N = 3$–4). $^{*}p < 0.05$ versus control

spindle-shaped or linear-shaped cells, which were indicated to be fibroblasts or myofibroblasts. Colocalization of Cygb and α-SMA was also observed in the linear-shaped cells, which confirmed the cells were myofibroblasts (third panel). Cygb was not expressed in the epithelial cells which were immunoreactive for cytokeratin (fourth panel).

Expression of HIF-1α and Cygb Protein in the Ulcerated Gastric Tissues

The sizes of gastric ulcer induced by acetic acid was 24.9 ± 2.9, 15.2 ± 2.7, 7.8 ± 0.5, 4.4 ± 0.6, and 1.4 ± 0.4 mm^2 on days 3, 7, 11, 18, and 25, respectively (Fig. 2a). These results were consistent with previous macroscopic and microscopic findings [24, 26]. Expression of HIF-1α protein in the ulcerated gastric tissues was significantly increased on day 7 after the production of gastric ulcer (1.83 ± 0.11 folds, $p < 0.05$ vs. control) and sustained up to day 11 (2.12 ± 0.19 folds, $p < 0.01$), which corresponded to the early phase of the healing stage (Fig. 2b). In contrast, Cygb protein was significantly increased on days 11 and 18 (1.87 ± 0.13 and 1.60 ± 0.06 folds, respectively, $p < 0.05$), which corresponded to the late phase of healing (Fig. 2c). Interestingly, HIF-1α was not significantly increased on day 18 whereas Cygb was increased. There was a difference between HIF-1α and Cygb protein expression in the time phase.

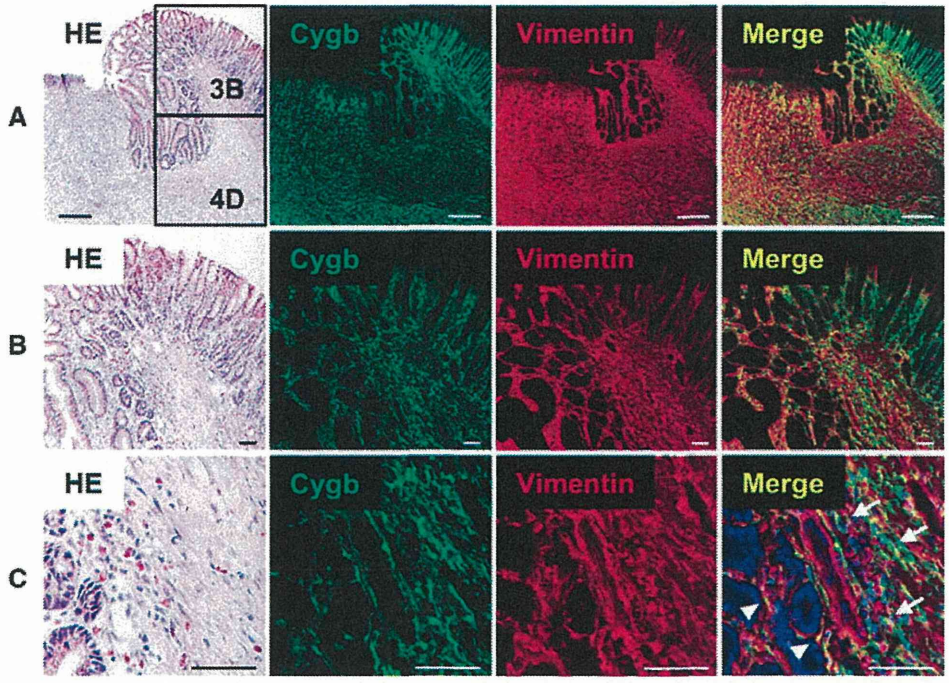

Fig. 3 Localization of Cygb in the ulcerated gastric tissues. **a** Cygb and vimentin expression in the ulcerated area. Cygb and vimentin were colocalized in the cytoplasm of mesenchymal cells in the regenerative area and the ulcer bed. **b** Middle magnified images. Colocalization was observed in the mucosal and submucosal layer. **c** Highly magnified images. Colocalization of Cygb and vimentin was observed in the spindle-shaped cells which were indicated to be fibroblasts (*arrows*). Colocalization was also observed in the linear-shaped cells surrounding the glands which were indicated to be myofibroblasts (*arrowheads*). *HE* hematoxylin and eosin. *Scale bars* **a** 250 μm; **b** and **c** 50 μm

mRNA Expression of HIF-1α and VEGF in the Ulcerated Gastric Tissues

mRNA expression of HIF-1α peaked on day 11 in the time course of ulcer healing (2.29 ± 0.56 folds, $p < 0.05$ vs. control; Fig. 2d). In contrast, VEGF expression was significantly increased on days 11 and 18 (1.02 ± 0.08 and 1.45 ± 0.31 folds, respectively, $p < 0.05$; Fig. 2e). VEGF mRNA expression was gradually increased from day 11 to 18. VEGF expression peaked at day 18.

Localization of Cygb in the Ulcerated Gastric Tissues

On day 11 after the ulcer production, Cygb and vimentin were colocalized in the cytoplasm of mesenchymal cells in the regenerative area and ulcer bed (Fig. 3a). In the regenerative area, immunoreactivity for Cygb was stronger than that in the ulcer bed. Colocalization was observed in the mucosal and submucosal layers (Fig. 3b). On highly magnified images, colocalization was observed in the spindle-shaped cells which were indicated to be fibroblasts (Fig. 3c). Furthermore, colocalization was also observed in the linear-shaped cells surrounding the glands which were indicated to be myofibroblasts. We could confirm the evidence that showed the linear-shaped cells represented myofibroblasts by colocalization of Cygb and α-SMA (Fig. 4a). Cygb was not expressed in the muscle cells which were positive for vimentin and α-SMA. Cygb was also not expressed in the epithelial cells which were immunoreactive for cytokeratin (Fig. 4b).

Localization of Cygb and HIF-1α in the Ulcerated Gastric Tissues

HIF-1α was expressed in the mucosal and submucosal layers at the marginal zone of the ulcer (Fig. 4c). Colocalization of Cygb and HIF-1α was stronger in the submucosal layer than that in the mucosal layer. On highly magnified images, colocalization was observed in the submucosal spindle-shaped cells which were indicated to be fibroblasts. Cygb protein, as well as HIF-1α, was observed at the regenerative tissues where angiogenesis had not developed at that time.

Association of Cygb With/Without Angiogenesis in the Ulcerated Gastric Tissues

The pattern of angiogenesis is different in the regenerative gastric tissues around the ulcer. Immunoreactive cells for Cygb were abundantly present at the regenerative tissues where immunoreactivity of HIF-1α was abundant (Fig. 4c). In contrast, immunoreactive cells for Cygb were sparsely

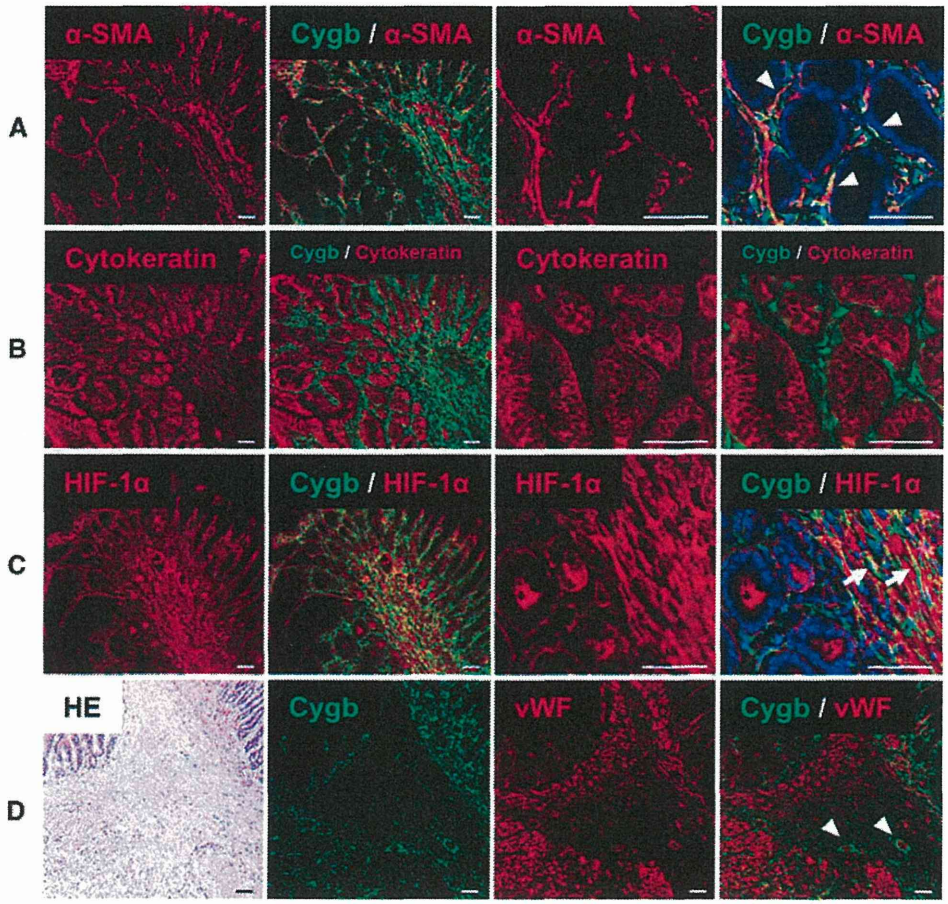

Fig. 4 Immunostaining for Cygb with α-SMA, cytokeratin, HIF-1α and vWF at the marginal zone of the ulcerated tissues. **a** Cygb and α-SMA expressions. Colocalization was observed in the mucosal layer (*first and second panel* from *left*). Highly magnified images showed double-positive cells were linear-shaped cells surrounding the glands which were indicated to be myofibroblasts (*third and fourth panel, arrowheads*). **b** Cygb and cytokeratin expressions. Cygb was not expressed in the epithelial cells which were immunoreactive for cytokeratin. Two panels from *left* are middle magnified and other panels are highly magnified images. **c** Cygb and HIF-1α expressions. HIF-1α was expressed in the mucosal and submucosal layer (*first panel* from *left*). Colocalization of Cygb and HIF-1α was stronger in the submucosal layer than that in the mucosal layer (*second panel*). On highly magnified images, colocalization was observed in the submucosal spindle-shaped cells which were indicated to be fibroblasts (*third and fourth panel, arrows*). **d** Cygb and vWF expressions. Cygb-immunoreactive cells were sparsely observed in the vicinity of vWF-immunoreactive vascular endothelial cells (*arrowheads*). *HE* hematoxylin and eosin. *Scale bars* 50 μm

observed in the vicinity of vascular endothelial cells (vWF-positive cells; Fig. 4d). Cygb was not expressed in the vascular endothelial cells. These results suggested that Cygb was upregulated at the regenerative tissues where angiogenesis had not occurred and it was still under hypoxic condition. However, immunoreactive cells for Cygb were sparse in the area where angiogenesis had already been developed.

Discussion

In this study, we showed that the expression of HIF-1α protein was significantly increased in the early healing phase of gastric ulceration (from day 7 to 11 after the production of gastric ulcer). In contrast, Cygb protein was significantly upregulated in the late healing phase of acute gastric mucosal injury and gastric ulceration (from day 11 to 18). There was a difference between HIF-1α and Cygb protein expression in the time phase. These results showed that Cygb was introduced after the HIF-1α protein stabilization. This is consistent with the previous report which showed that Cygb was regulated by HIF-1α [4, 11]. We finally considered that the healing phase could be divided into two phases; phase 1, early phase (HIF-1α elevating phase, from day 7 to 11); phase 2, late phase (Cygb elevating phase, from day 11 to 18).

Concerning the localization of Cygb, we demonstrated that Cygb was expressed on fibroblasts and myofibroblasts. Cygb was not expressed in the epithelial cells. These results were commonly observed in both an acute gastric mucosal injury model and chronic gastric ulcer model. Moreover, double positive spindle shaped cells for Cygb and HIF-1α were abundantly present at the marginal zone of gastric ulcer, whereas Cygb-immunoreactive cells were not observed in the vicinity of vWF-positive cells. Cygb expression was faint in the regenerative tissues with angiogenesis. From day 11 to 18, Cygb and HIF-1α protein levels were gradually decreased from the peak level observed at day 11. However, VEGF mRNA level was increased in a time-dependent manner from day 11 to 18. VEGF expression peaked at day 18. These characteristic changes of HIF-1α and VEGF expressions during gastric ulcer healing are consistent with the previously reported data [15]. These results suggest that the area with angiogenesis which is mediated by VEGF has not already been under hypoxic condition. In contrast, a hypoxic condition in the ulcerated area triggers HIF-1α induction followed by Cygb induction in the mesenchymal cells like fibroblasts. Accordingly, Cygb is likely to function as a transit oxygen supplier, oxygen sensor, and scavenger of reactive oxygen species in the relatively hypoxic lesion in which angiogenesis has not been completed. Cygb functions as an intracellular oxygen transporter because this protein has 40 % amino acid sequence homology with myoglobin [7]. Fago et al. [6] demonstrated that O_2 binding to Cygb was pH-independent and exothermic throughout the temperature range investigated. These results showed that Cygb might be involved in O_2-requiring metabolic processes. Previous reports showed Cygb might function as a scavenger of reactive oxygen species [4, 5]. Xu et al. [27] demonstrated that an increased expression of Cygb in hepatic stellate cells protected the cells from oxidative stress when exposed to nitrolotriacetate and arachidonic acid, two compounds which induced lipid peroxidation. Besides the heme, other components may also contribute to scavenging for reactive oxygen species (ROS), like reactive thiols, which are readily accessible to oxidizing agents. The exact mechanism by which Cygb protects the cell against oxidative stress-induced cell death remains to be elucidated. In addition, Cygb triggers the transformation of fibroblasts to myofibroblasts that express well-developed actin stress fibers and stimulates collagen production at the inflammatory sites [3]. The extracellular matrix (ECM), including collagen, fibronectin, and laminin, plays an important role in cell adhesion, migration, and proliferation during wound healing [28, 29]. Cygb is associated with ECM synthesis in the healing process and the present time course of Cygb expression was consistent with those of ECM expression needed for ulcer healing in our previous report [24]. Cygb may also play a role as an introducer of tissue fibrosis during the late phase of gastric ulcer healing. Unfortunately we could not investigate the precise role of Cygb in this study. Though Cygb and HIF-1α were colocalized in the cytoplasm of the spindle-shaped cells, there is no direct evidence to indicate that HIF-1α binds to HRF motifs of the *CYGB* gene. Further studies are needed to clarify these problems.

In conclusion, Cygb was mainly expressed on myofibroblasts and fibroblasts and it may be involved in the healing process of gastric mucosal injuries in the late phase when angiogenesis has not been developed. This finding may be helpful for elucidating the mechanism(s) underlying the healing process. Cygb targeting therapy may provide a new strategy for the treatment of various ulcerative diseases.

Conflict of interest None.

References

1. Kawada N, Kristensen DB, Asahina K, et al. Characterization of a stellate cell activation-associated protein (STAP) with peroxidase activity found in rat hepatic stellate cells. *J Biol Chem.* 2001;276:25318–25323.
2. Asahina K, Kawada N, Kristensen DB, et al. Characterization of human stellate cell activation-associated protein and its expression in human liver. *Biochim Biophys Acta.* 2002;1577:471–475.
3. Nakatani K, Okuyama H, Shimahara Y, et al. Cytoglobin/STAP, its unique localization in splanchnic fibroblast-like cells and function in organ fibrogenesis. *Lab Invest.* 2004;84:91–101.
4. Fordel E, Thijs L, Moens L, Dewilde S. Neuroglobin and cytoglobin expression in mice. Evidence for a correlation with reactive oxygen species scavenging. *FEBS J.* 2007;274:1312–1317.
5. Mammen PP, Shelton JM, Ye Q, et al. Cytoglobin is a stress-responsive hemoprotein expressed in the developing and adult brain. *J Histochem Cytochem.* 2006;54:1349–1361.
6. Fago A, Hundahl C, Dewilde S, Gilany K, Moens L, Weber RE. Allosteric regulation and temperature dependence of oxygen binding in human neuroglobin and cytoglobin. Molecular mechanisms and physiological significance. *J Biol Chem.* 2004;279:44417–44426.
7. Burmester T, Ebner B, Weich B, Hankeln T. Cytoglobin: a novel globin type ubiquitously expressed in vertebrate tissues. *Mol Biol Evol.* 2002;19:416–421.
8. Hankeln T, Ebner B, Fuchs C, et al. Neuroglobin and cytoglobin in search of their role in the vertebrate globin family. *J Inorg Biochem.* 2005;99:110–119.
9. Schmidt M, Gerlach F, Avivi A, et al. Cytoglobin is a respiratory protein in connective tissue and neurons, which is up-regulated by hypoxia. *J Biol Chem.* 2004;279:8063–8069.
10. Fordel E, Geuens E, Dewilde S, et al. Cytoglobin expression is upregulated in all tissues upon hypoxia: an in vitro and in vivo study by quantitative real-time PCR. *Biochem Biophys Res Commun.* 2004;319:342–348.
11. Guo X, Philipsen S, Tan-Un KC. Study of the hypoxia-dependent regulation of human CYGB gene. *Biochem Biophys Res Commun.* 2007;364:145–150.

12. Ferrara N. Role of vascular endothelial growth factor in regulation of physiological angiogenesis. *Am J Physiol Cell Physiol.* 2001;280:C1358–C1366.
13. Takahashi M, Kawabe T, Ogura K, et al. Expression of vascular endothelial growth factor at the human gastric ulcer margin and in cultured gastric fibroblasts: a new angiogenic factor for gastric ulcer healing. *Biochem Biophys Res Commun.* 1997;234:493–498.
14. Jones MK, Itani RM, Wang H, et al. Activation of VEGF and Ras genes in gastric mucosa during angiogenic response to ethanol injury. *Am J Physiol.* 1999;276:G1345–G1355.
15. Hashimoto H, Akimoto M, Maeda A, Shigemoto M, Yamashito K. Relation of hypoxia-inducible factor-1alpha to vascular endothelial growth factor and vasoactive factors during healing of gastric ulcers. *J Cardiovasc Pharmacol.* 2004;44:S407–S409.
16. Forsythe JA, Jiang BH, Iyer NV, et al. Activation of vascular endothelial growth factor gene transcription by hypoxia-inducible factor 1. *Mol Cell Biol.* 1996;16:4604–4613.
17. Salceda S, Caro J. Hypoxia-inducible factor 1alpha (HIF-1alpha) protein is rapidly degraded by the ubiquitin-proteasome system under normoxic conditions. Its stabilization by hypoxia depends on redox-induced changes. *J Biol Chem.* 1997;272:22642–22647.
18. Ito M, Tanaka S, Kim S, et al. The specific expression of hypoxia inducible factor-1alpha in human gastric mucosa induced by nonsteroidal anti-inflammatory drugs. *Aliment Pharmacol Ther.* 2003;18:90–98.
19. Baatar D, Jones MK, Tsugawa K, et al. Esophageal ulceration triggers expression of hypoxia-inducible factor-1 alpha and activates vascular endothelial growth factor gene: implications for angiogenesis and ulcer healing. *Am J Pathol.* 2002;161:1449–1457.
20. Semenza GL, Jiang BH, Leung SW, et al. Hypoxia response elements in the aldolase A, enolase 1, and lactate dehydrogenase A gene promoters contain essential binding sites for hypoxia-inducible factor 1. *J Biol Chem.* 1996;271:32529–32537.
21. Watanabe T, Higuchi K, Hamaguchi M, et al. Monocyte chemotactic protein-1 regulates leukocyte recruitment during gastric ulcer recurrence induced by tumor necrosis factor-alpha. *Am J Physiol Gastrointest Liver Physiol.* 2004;287:G919–G928.
22. Taira K, Watanabe T, Tanigawa T, et al. Roles of cyclooxygenase-2 and prostaglandin E receptors in gastric mucosal defense in Helicobacter pylori-infected mice. *Inflammopharmacology.* 2007;15:132–138.
23. Okabe S, Roth JL, Pfeiffer CJ. A method for experimental, penetrating gastric and duodenal ulcers in rats. Observations on normal healing. *Am J Dig Dis.* 1971;16:277–284.
24. Tominaga K, Arakawa T, Kim S, Iwao H, Kobayashi K. Increased expression of transforming growth factor-beta1 during gastric ulcer healing in rats. *Dig Dis Sci.* 1997;42:616–625.
25. Hayakawa T, Fujiwara Y, Hamaguchi M, et al. Roles of cyclooxygenase 2 and microsomal prostaglandin E synthase 1 in rat acid reflux oesophagitis. *Gut.* 2006;55:450–456.
26. Uchida M, Kawano O, Misaki N, Saitoh K, Irino O. Healing of acetic acid-induced gastric ulcer and gastric mucosal PGI2 level in rats. *Dig Dis Sci.* 1990;35:80–85.
27. Xu R, Harrison PM, Chen M, et al. Cytoglobin overexpression protects against damage-induced fibrosis. *Mol Ther.* 2006;13:1093–1100.
28. Grinnell F, Billingham RE, Burgess L. Distribution of fibronectin during wound healing in vivo. *J Invest Dermatol.* 1981;76:181–189.
29. Kurkinen M, Vaheri A, Roberts PJ, Stenman S. Sequential appearance of fibronectin and collagen in experimental granulation tissue. *Lab Invest.* 1980;43:47–51.

EXPERT OPINION

informa
healthcare

A mouse with humanized liver as an animal model for predicting drug effects and for studying hepatic viral infection: where to next?

Katsutoshi Yoshizato† & Chise Tateno
Phoenixbio - Academic Adviser Office, Hiroshima, Japan

Introduction: The mouse is a common model used in evaluating drug metabolism and hepatitis infectivity. However, these models have limited value due to species difference in hepatic functions, leading to the creation of the chimeric mouse 12 years ago. These models were unique in that their hepatocytes had been replaced with human (hu) hepatocytes (dubbed the 'first-generation chimeric mouse'). Since then, the chimeric mouse has become a practical tool for this area of studies. However, some shortcomings have also been recognized. One major shortcoming is that the mouse cannot mimic hu-liver diseases due to immunodeficiency and also it is unable to provide sufficient amounts of blood for analysis compared to the rat. There are also issues around donor-to-donor variability of hu-hepatocytes such as variable engraftment efficiency.

Areas covered: This review provides the current status of the first-generation chimeric mouse. Furthermore, the authors review studies intended to create a 'second-generation of the chimeric mouse' in which inflammation/immune-response cells as well as hepatocytes are humanized. A brief comment is also made on studies aiming at producing chimeric rats. Finally, the authors consider induced pluripotent stem cells (iPS cells) as new sources of hu-hepatocytes.

Expert opinion: The authors believe that the current rapid progress in the field of biotechnology should enable us to create a mouse model with a humanized liver that is made by iPS-derived hu-hepatocytes and hu-immune cells. This development will provide researchers with a model that will be able to effectively mimic human liver disease under experimental conditions.

Keywords: chimeric mouse, drug testing, hepatitis infection model, mouse with humanized liver

Expert Opin. Drug Metab. Toxicol. [Early Online]

1. Introduction

Ideal drugs and medicines are defined as natural or artificial substances that are effective at improving disease conditions in humans without inducing any harmful outcomes. Tremendous efforts and costs are required for pharmaceutical companies to successfully produce such drugs for public use. Conventionally, rodents, usually rats and mice, have been utilized for research and development (R&D) of new drugs and medicines. However, there are often cases in which such candidates fail to exhibit the effects and safety predicted from the animal experiments during

10.1517/17425255.2013.826649 © 2013 Informa UK, Ltd. ISSN 1742-5255, e-ISSN 1744-7607

Article highlights.

- Humanization of the mouse liver has greatly benefited drug metabolism prediction in humans.
- Mice with humanized liver have also proven to be a precious tool to study infection and proliferation of hepatitis viruses.
- Human hepatocytes propagated in humanized mice could prove to be a useful source of human hepatocytes for *in vitro* drug-testing.
- Mice with humanized liver and immune/inflammation systems will be available and could capture the effects of hepatitis and hepatic fibrogenesis when their livers are exposed to stress.
- Technologies for creating humanized mice using human iPS cells will be available, in the future, and these will increase the utility of humanized mice for drug testing.

This box summarizes key points contained in the article.

preclinical tests. This phenomenon occurs because rodents are not necessarily identical to humans regarding the metabolic and toxicological profiles of drugs (species differences).

Generally, R&D consists of two types of studies: preclinical and clinical trials of candidate drugs, which represent testing in animals or *in vitro* (with cultured cells) and in humans, respectively [1,2]. Data concerning the drug's feasibility and safety pharmacodynamics are collected during preclinical development. It is said that the success rate of tested compounds that gain approval is ~ 10% [3]. However, the number of drugs that can survive for a sufficient period of time as drugs for public use is quite few; the success rate in this sense is estimated to be as low as < 0.01% [4]. As a whole, one of the major causes of these failures is the unpredictability of efficacy in animal models due to rodent–human species differences. Therefore, the development of accurately predictable animal models is greatly required in pharmaceutical areas. The liver is the prime site of drug metabolism of orally administered drugs, which predominantly express genes of the three cytochrome P450 (CYP450) families (CYP1, CYP2 and CYP3) [5], the prime contributors for eliminating most clinical drugs [6].

There have been two straightforward approaches to decrease the mouse (m)–human (hu) species differences in drug metabolism and to increase the predictability of metabolic profiles of a given test drug based on data from mouse studies. One is to create mice in which major hu-genes involved in drug metabolism such as those of CYPs are incorporated (gene-humanized [*h*] mice). The other is to create a mouse (the so-called a chimeric mouse) with the liver in which hepatic parenchymal cells (hepatocytes) are replaced with hu-counterparts. The present review focuses on the hepatocyte-*h*-mouse and describes its present status with regard to the methodology to generate them, the advantages and limitations in their usage and the necessity of methodological developments to generate a new type of *h*-mice that could solve the problems associated with the currently available chimeric mice. Reviews are available to readers who are interested in the gene-*h*-mouse [7,8]. A review is also available that comparatively summarizes the present status of studies of both gene- and hepatocyte-*h*-mice [9].

The first chimeric mouse was created in 2001 as a m-model for studying the mechanisms of infection and the propagation of hu-hepatitis viruses [10,11]. Methodological improvements enabled us to reproducibly and stably generate chimeric mice at high levels of chimerism and in sufficient numbers for preclinical tests [12]. As a result, these mice have often been utilized in medical and pharmaceutical studies, and much knowledge has been accumulated regarding their usefulness and limitations. Several attempts have been made to improve the methods for producing chimeric mice, and new technology to manipulate hu-cells has been developed since the advent of the chimeric mouse. These situations have enabled researchers to create a new type of liver-*h*-mouse, in which not only hepatocytes but also blood cells responsible for inflammation and immune reactions are humanized (liver with dual chimerism). The original and new types of *h*-mouse are dubbed 'first-generation' and 'second-generation' chimeric mice, respectively, in this review. Previously, we reviewed the characteristics of the first-generation chimeric mice mainly focusing on the growth of hu-hepatocytes, the interactions between hu-hepatocytes and host non-parenchymal cells, drug metabolism and the propagation of hepatitis viruses [13-16]. In the present article, the current status of the first-generation chimeric mouse is reviewed with special emphasis on studies to overcome its limitations. We also comment on hu-induced pluripotent stem cells (iPS cells) as a cell type of great promise for a new source of hu-hepatocytes.

2. Requirements for the host to be hepatocyte-humanized

Hepatocyte-humanization requires two features of a mouse as host. First, the host must be immunodeficient, which allows it to accept xenogeneic cells when properly transplanted. Second, its hepatocytes must be damaged, which allows xenogeneic hepatocytes to engraft and colonize the host liver by proliferating at the expense of the host's damaged counterpart cells [17]. Thus far, four types of hepatocyte-*h*-mice have been developed as the major first-generation models, which differ from each other in the ways of conferring a combination of immunodeficiency and hepatocytic injury on the host mouse. Two research groups independently generated the first workable hepatocyte-*h*-mice in 2001 [10,11]. Regarding the immunodeficiency requirement, one group [10] used recombination-activating gene-2 (Rag-2)-knockout (KO) mice, and the other [11] adopted severe-combined immunodeficient (SCID) mice as reported by Bosma *et al.* [18]. The mature B and T lymphocytes play key roles in the adaptive immune system. Developing lymphocytes restrictedly express two RAG product enzymes, known as RAG1 and RAG2, which play an

important role(s) in the rearrangement and recombination of the genes of immunoglobulin and T-cell receptor molecules during the process known as VDJ recombination [19]. Thus, RAG1 and RAG2 are crucial to the generation of mature B and T cells. The former group utilized this mechanism of differentiation of lymphocytes and chose mice with a $Rag2^{-/-}$ background but not those with a $Rag1^{-/-}$ background [10]: it was reported that hu-hepatocytes did not successfully repopulate the damaged liver of $Rag1^{-/-}$ mice in which fumarylacetoacetate hydrolase (FAH) gene had been deleted [20]. As described below, the absence of the Fah gene leads to an accumulation of toxic tyrosine catabolites within the hepatocytes. $Rag2^{-/-}$ mice (Balb/C-line) were also excellent recipients of hu-hematopoietic xenografts when combined with Il2rg-deficiency [21,22]. The $Rag2^{-/-}$ mice lack mature lymphocytes due to their inability to initiate VDJ rearrangement [23]. SCID mice also lack mature B and T cells due to an inactivating mutation in the catalytic subunit of a DNA-dependent protein kinase ($Prkdc^{scid}$) [24], but other hematopoietic cell types develop and function normally, including monocytes/macrophages, neutrophils, natural killer (NK) cells and dendritic cells (DCs) [25].

Later, an additional immunodeficient m-strain, NOG, was utilized as a host. These mice lack not only mature T and B lymphocytes but also NK cells [26]. Non-obese diabetic (NOD) mice are known to exhibit the spontaneous development of autoimmune insulin-dependent diabetes mellitus [27], and NOD-related strains were developed at the Shionogi Research Laboratories as NOD/Shi mice. NOD/Shi mice were crossed with the SCID mice, the offspring (NOD/Shi-*scid*) of which were mated with interleukin-2 receptor g-chain gene-KO (C57BL/6J-IL-$2Rg^{null}$) mice. The resulting m-strain is highly immunodeficient and is called NOG (NOD/Shi-*scid* IL-$2Rg^{null}$) [28].

Regarding the requirement of hepatocyte damage, genetically liver-injured m-line, albumin (Alb) promoter/enhancer-driven urokinase-type plasminogen activator (Alb-uPA) gene-transgenic ($Tg_{Alb\text{-}uPA}$) mice were originally developed to generate mice with damaged livers. This line carries a tandem array of four murine urokinase genes [29] and has long been utilized to generate hepatocyte-*h*-chimeric mice. The mice of this line are mated with one of the above three types of immunodeficient mice strains (Rag-2-KO, SCID and NOG). The liver of the $Tg_{Alb\text{-}uPA}$ mouse becomes severely hypofibrinogenemic after birth because the hepatocytes of $Tg_{Alb\text{-}uPA}$ mice overproduce urokinase under the control of the Alb promoter/enhancer, which accelerates death of hu-hepatocytes through multiple undefined mechanisms involving extracellular matrix decomposition [30]. Fah has also been utilized as a hepatocyte-damaging agent. In previous studies, mice were triple-mutated for Fah, Rag2, and the common g-chain of the interleukin receptor ($Fah^{-/-}/Rag^{2-/-}/Il2rg^{-/-}$ mice) [20,31]. These mice lack B-, T- and NK-cells, and, thus, their immunodeficiency is more complete compared to $Rag^{2-/-}$ or SCID mice. The hepatocytes of these mice are damaged due to the absence of the Fah gene, which leads to an accumulation of toxic tyrosine catabolites within the hepatocytes [32]. This genetically determined toxicity is preventable by oral administration of 2-(2-nitro-4-trifluoro-methylbenzoyl)-1,3-cyclohexane-dione (NTBC), which blocks hydroxyphenylpyruvate dioxygenase activity upstream of Fah and therefore prevents the accumulation of hepatotoxic metabolites. As noted above, when hu-hepatocytes are introduced to damaged livers in uPA-Tg- or $Fah^{-/-}$-mice, the donor cell chimerism takes place exclusively in the liver, because first hu-hepatocytes exhibit high affinity to their original (liver) tissues, and second damages are induced exclusively in the liver in these gene-manipulated model animals.

To date, the immunodeficient uPA mouse has been best characterized and most frequently utilized as the host for xenogenic hepatocyte transplantation. A high level of hu-chimerism can be obtained when homozygous uPA mice are used as hosts, though these mice suffer from infertility. There is a method to overcome this disadvantage. A research group transplanted healthy non-Tg-m-hepatocytes into uPA homomice [33]. As a result, the group found that their livers were totally repopulated with the normal hepatocytes, and importantly, the mice themselves became normal in body weight, life span and fertility. Fah-deficient mice are said to have some advantages over uPA-overexpressing mice [20]. In the former, the time and extent of liver disease are controllable by administering and withdrawing NTBC12 depending on an investigator's study design. The former m-line contains a Fah gene deletion, and thus it does not revert back to wild-type by transgene inactivation, which is often problematic in the latter m-line [34]. Originally, we administered a complement inhibitor during the establishment processes of the hepatocyte-*h*-mice with the uPA/SCID background [12], which could be a potential source of pharmacological interference and limits their usage in virological applications. However, currently established lines of uPA-Tg/SCID mice are able to accept hu-hepatocytes at high levels of replacement (replacement index [RI] > 80% in average, the ratio of the repopulated hu-hepatocytes to the total number of host (m)- and hu-hepatocytes in the host liver) without treatment of the complement inhibitor. The possibility of cell fusion in the hu-hepatocyte repopulation process could not be ruled out in uPA-overexpressing mice [20,] because liver repopulation by embryoid body-derived monkey hepatocytes in uPA-Tg-mice was due almost entirely to cell fusion between the hu- and m-hepatocytes [35]. However, in our accumulated experiences, such cell fusion has never been observed in hematoxylin and eosin-stained histological examinations in which m-hepatocytes were clearly distinguishable by their intense eosinophilicity in the hepatocyte-*h*-mouse. These host hepatocytes were all single cells, degenerative, and did not locate in the regions where hu-hepatocytes were repopulated in the form of nodules [12]. These repeated and reproducible histological observations accumulated to date enable us to rule out the possibility of cell fusion or to conclude that if fused cells exist, they are rare.

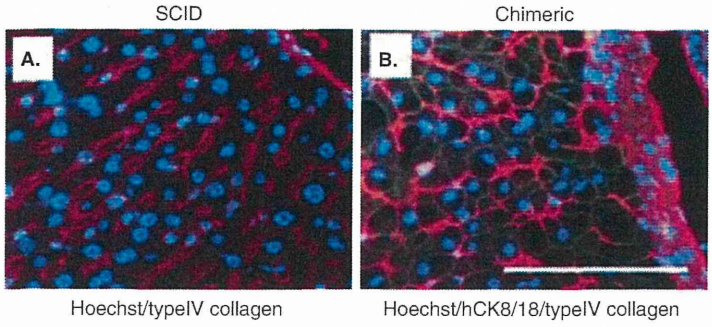

Figure 1. Illustration of assembly of hu-hepatocytes in a twin-cell plate fashion in the chimeric m-liver. Liver tissues of SCID mice were subjected to Hoechst staining (blue) and immunostaining for type IV collagen (red) (**A**). Similarly, liver tissues isolated at 13 - 15 weeks post-transplant from chimeric mice with 5-year-old male hepatocytes were subjected to Hoechst staining (blue), immunostaining for type IV collagen (red) and hu-specific CK8/18 (yellow) (**B**). The m-hepatocytes in SCID m-liver are organized in a single-cell plate fashion, but hu-hepatocytes in chimeric m-liver are organized in a twin-cell plate fashion, reflecting their highly proliferative potential as reported previously [75]. Bar represents 100 μm.
Reproduced from [36] with the permission of Nature Publishing Group.

3. Hepatocyte-humanized mouse and its utilization

When transplanted, hu-hepatocytes engraft and actively colonize the livers of immunodeficient and liver-injured mice [12]. In the 8 years of experience, since the original report in 2004 [12], many improvements have been made in our hepatocyte-*h*-mouse-producing system, and, as a result, the chimeric mice in our facility usually attain RI > 90%, ~ 2 months after transplantation [13]. Recently, *h*-livers in this model that had been produced by transplanting hu-hepatocytes from 2- to 10-year-old males or females to 2- to 4-week-old homozygotic uPA/SCID mice were characterized in details with respect to morphology and gene expression profiles [36], which is summarized as follows. The hu-Alb monitoring in host blood was performed in 54 mice with 5-year-old male hepatocytes for 8 - 16 weeks following transplant. Of these animals, 50 remained alive beyond 10 weeks of age (> ~ 7 weeks post-transplantation). Most of the surviving hosts (~ 90%) secreted > 7 mg/ml hu-Alb into the blood at 8 - 16 weeks after the transplant, indicating RIs > ~ 75%. The hepatocytes and their nuclei were smaller in the chimeric mice than in the SCID mice, as are those in a hu-body. Type IV immunostaining showed that hu-hepatocytes in the *h*-mice are arranged in a manner of 'twin-cell' plates and not in single-cell plates as in normal livers (**Figure 1**).

The occupancy of parenchymal cells (mostly hu-hepatocytes) in the chimeric m-liver was higher (~ 2-fold) compared to that of m-hepatocytes in the SCID m-liver. A fluorescent probe (indocyanine green) was injected into the mice to determine the blood flow in the liver. Blood was collected at appropriate time points after injection to determine the concentrations of the probe. The data obtained showed that there was no difference in the overall blood flow within the liver between chimeric and SCID mice, but the blood cell flow rate in the sinusoids was slower (~ 50%) in the chimeric m-liver than in SCID m-liver, which might be explained by the enlargement (> ~ 2-fold) of the former liver compared to the latter liver. No disturbance of the microcirculation was observed in the chimeric m-liver despite the slower sinusoidal blood cell flow. The hu-hepatocytes in the chimeric m-liver were not found in conditions of hypoxia, but were found in conditions of normoxia in spite of the lower blood cell flow. This result might be related to the fact that the oxygen consumption rate of hu-hepatocytes in the chimeric m-liver was slower (~ 20%) than that of m-hepatocytes in SCID m-liver, although the rate was still higher (~ 2-fold) than that of the donor hepatocytes. Microarray profiles showed that ~ 80% of the ~ 16,600 tested probes were within a twofold range difference between hu-hepatocytes in the chimeric m-livers and those in hu-livers. Immunohistochemical and electron microscopic examinations of the chimeric m-liver showed normal construction of the sinusoids by hu-hepatocytes and m-hepatic sinusoid cells (Kupffer cells, stellate cells and sinusoidal endothelial cells), as detailed in **Figure 2**.

Hepatocyte-*h*-mice exhibiting such characteristics described above are becoming a general tool in laboratories to understand and characterize hu-livers. We first demonstrated that the *h*-m-liver mimics hu-phenotypes at a level appropriate for pharmacological studies, and thus, these hepatocyte-*h*-mice can be used not only for developing new medicines but also for examining biological and pathological mechanisms in the hu-liver, including hepatitis infection and propagation.

3.1 Drug testing and screening

We demonstrated that the expression profiles of major CYPs involved in Phase I drug metabolism by hu-hepatocytes of the *h*-mice are similar to those of donors and are inducible

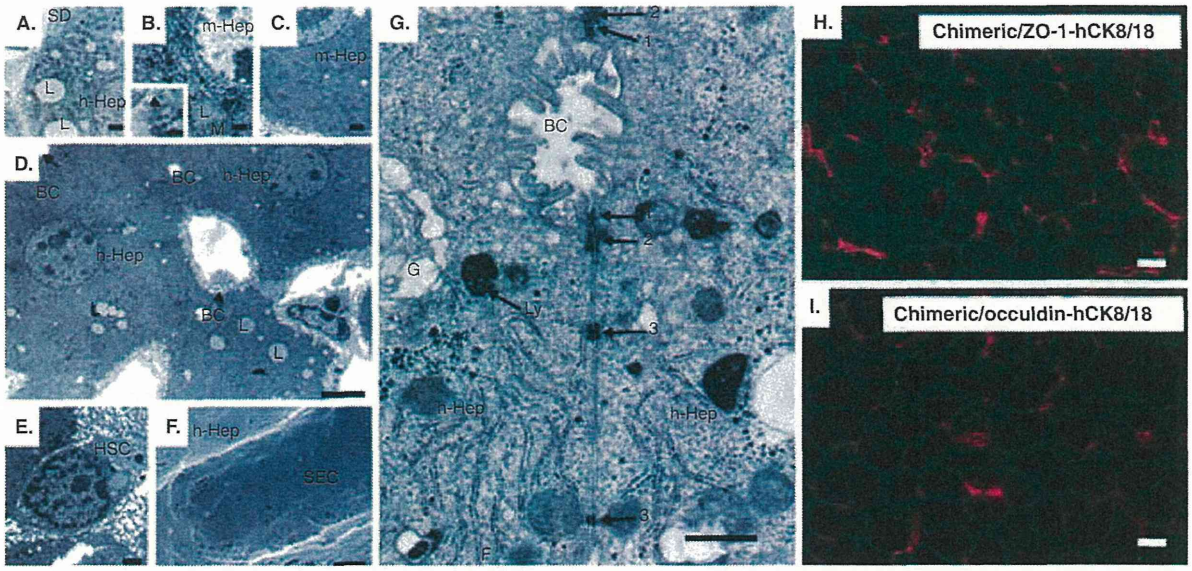

Figure 2. Illustration of structural features of chimeric m-liver. The *h*-regions of a chimeric m-liver were characterized with electron microscopy compared to non-*h*-regions in the same individual. Liver tissues were examined by transmission electron microscopy (**A** – **E, G**), scanning electron microscopy (**F**) and immunohistochemistry (**H** and **I**). Histochemical sections from chimeric liver tissues were stained for ZO-1 and hCK8/18 (**H**) and for occuldin-1 and hCK8/18 (**I**). The hu-hepatocytes in the *h*-regions are featured by the presence of abundant glycogen and large lipid droplets in the cytoplasm (**A**). The m-hepatocytes that retain the transgene (uPA gene) are diseased and contain abundant small granules (**B**). The m-hepatocytes that lose the uPA gene become normal (**C**). Normal sinusoidal structures are elaborated by hu-hepatocytes and m-non-parenchymal cells as seen in (**A**), in which the space of Disse is clearly discernible. The hu-hepatocytes adhere to each other and form bile canaliculi on the apical surface (**D**). The basal surfaces of hu-hepatocytes develop abundant microvilli, facing the thin m-sinusoidal endothelial cells (**D**), which are fenestrated (**F**). A hepatic stellate cell with lipid droplets is shown in the space of Disse (**E**). Bile canaliculi are organized by junctional complexes, consisting of tight junctions, adherence junctions and desmosomes (**G**). Tight junction proteins such as ZO-1 (**H**) and occludin-1 (**I**) are involved in these adhesions. Occasionally, bile canaliculi are also formed between hu- and m-hepatocytes (**G**). Bar represents 1 μm in (**A** – **C, E, F**); 5 μm in (**D**); 10 μm in (**H**) and (**I**); 0.5 μm in (**G**).
Reproduced from [36] with the permission of Nature Publishing Group.
BC: Bile canaliculi; BL: Blood cell; HSC: Hepatic stellate cell; L: Lipid droplets; M: Mitochondria; SD: Sinusoid; SEC: Sinusoidal endothelial cell; G: Golgi complex; Ly: Lysosome.

by known CYP species-specific drugs [13,15,16]. Similarly, major enzymes involved in Phase II drug metabolism, such as uridine 5′-diphospho-glucuronosyltransferase (UGT), sulfotransferase (SULT), *N*-acetyltransferase (NAT), and glutathione *S*-transferase, are appreciably expressed in hu-hepatocytes [13]. These Phase II enzymes are known to participate in the metabolism of a drug group that bind to PXRs or constitutive androstane receptors, allowing these receptors to regulate some Phase II enzyme genes on ligation with drugs. Human-type Phase II metabolism is thought to function in these mice because a study showed that a conjugated form of a metabolite of an anabolic steroid, metandienone, which is known to be processed through Phase II (conjugation), was detected in chimeric m-urine [37]. The capacity of drugs to be transported through the hepatocyte cell membrane is an essential feature of effective drugs, and this consists of recognition and intake of drugs as well as secretion of the drugs. The extrahepatic-to-hepatic transportation that is responsible for drug recognition and intake is performed by transporters, such as organic cation transporter 1, organic anion transporting polypeptide (OATP) 1B1 and OATP1B3. Adenosine 5′-triphosphate-binding cassette (ABC) proteins are responsible for hepatic-to-bile-duct transportation, which occurs in drug excretion. Currently available data indicate that these drug transporter systems are also humanized in the chimeric mouse, although the data related to humanization of hepatic drug transportation are quite limited [13].

To determine whether the *h*-chimeric mouse may be utilized as a m-model to examine the excretory pathway of a drug, a study was conducted using cefmetazole as a probe drug, which in humans is mainly excreted in the urine [38]. Non-*h*-mice (uPA$^{wild/wild}$/SCID mice) excreted 23.7 and 59.4% of the drug in urine and feces, respectively. In contrast,